A novel model reference adaptive control approach investigation for power electronic converter applications

Electrical Power and Energy Systems 156 (2024) 109722

Contents lists available at ScienceDirect

International Journal of Electrical Power and Energy Systems

journal homepage: www.elsevier.com/locate/ijepes

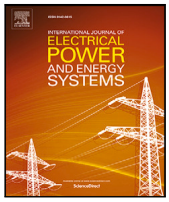

A novel model reference adaptive control approach investigation for power electronic converter applications

Muhammad Ahmed Qureshi [a], Salvatore Musumeci [a], Francesco Torelli [b], Alberto Reatti [c], Andrea Mazza [a], Gianfranco Chicco [a,*]

[a] Dip. Energia "Galileo Ferraris", Politecnico di Torino, Torino, Italy
[b] Dip. Ing. Elettrica e dell'Informazione, Politecnico di Bari, Bari, Italy
[c] Dip. Ingegneria dell'Informazione, University of Florence, Florence, Italy

ARTICLE INFO

Keywords:
Power converter
Model reference
Tracking control
Lyapunov theory
Sensitivity theory
Torelli control box
Regulation
Stability
Buck converter
Boost converter

ABSTRACT

This paper demonstrates the viability and effectiveness of a novel adaptive control approach applied to power electronic converters. A methodology based on the formulation of a Lyapunov-based approach is showcased to represent the operation of a new adaptive controller for the regulation of two power converter topologies (Buck and Boost). The models of the Buck and Boost converter topologies include the parasitic parameters that represent the non-ideal components. The basic idea of the control approach is to demonstrate adaptive stabilization for the proposed non-linear system. The most important design specification to stabilize the system is to track the reference trajectory in such a way that the error on the output variable converges asymptotically to zero. This adaptation mechanism is explicitly designed so that the asymptotic stability of the equilibrium condition is guaranteed according to the Lyapunov theorem and sensitivity theory. The details of the design algorithm are explained in the paper. The proposed control approach has been compared to other Lyapunov-based control techniques proposed in literature for the same non-ideal converters. The results show that the proposed controller provides better level of robustness and performance than the other well-established Lyapunov based controllers. To verify the effectiveness of the controller in real time, a test bench has been set up with prototypes of both converters and the controller has been implemented using the Arduino microcontroller and the control system driven through the Matlab/Simulink platform.

1. Introduction

In the power electronics area with the operation of the circuits in direct current (DC), numerous applications ranging from communication systems and consumer electronics to industrial electronics and DC energy networks use DC–DC power converters to regulate the DC voltage level. Switched-mode DC–DC power converters are widely used in power electronics for energy conversion systems, in different cutting-edge applications such as battery chargers for traction or energy-storage systems [1], photovoltaic (PV) and fuel cells voltage regulator [2], uninterruptible power supply [3], LED driver circuits [4], and so forth. DC–DC power converter topologies are developed considering higher efficiency, reliable control switching strategies, and fault-tolerant configurations for an extensive range of power [5,6]. Furthermore, the power converter configuration is divided into isolated and non-isolated circuital topologies [7]. Several power electronic switches are involved in the converter circuit development depending on the voltage requested and the power rate in pure Silicon (Si) technologies such as MOSFET, IGBT, GTO and IGCT [8,9] or wide bandgap (WBG) devices as Silicon Carbide (SiC) MOSFET or Gallium Nitride (GaN) FET devices [10,11]. The selection of power electronic devices is a crucial design point to optimize the dynamic performances and the converter efficiency. The choice of the electronic components influences the switch device parameters used in converter modelling.

The Boost, Buck, and Buck–Boost converters are the basic, most used non-isolated topologies. Therefore, many types of power electronics research in DC–DC conversion applications are carried out on these converter circuits [12]. The modelling of the converter circuit is used to design the converter operation and the control strategies. Mathematically speaking, the structure of a DC–DC power converter can be categorized as belonging to a class of systems that can be described as variable structure systems [13]. This is because the DC–DC power converter contains switching components and their dynamics at any given point in time are dependent on the state of the switch. Several modelling approaches are reported in the literature for the basic

* Corresponding author.
E-mail address: gianfranco.chicco@polito.it (G. Chicco).

https://doi.org/10.1016/j.ijepes.2023.109722
Received 28 December 2022; Received in revised form 22 October 2023; Accepted 12 December 2023

converter topologies, control strategies, and applications. In [14], a small-signal model of a Pulse Width Modulation (PWM) Boost converter is used to investigate the circuit operation and performance. A graphic methodology is used to achieve a model of the Buck–Boost converter, and the controller is used on the model [15]. Sliding mode and fuzzy logic Maximum Power Point Tracking (MPPT) techniques are applied to a Boost converter: the modelling approach is used to describe the control methods in the PV system [16].

The inherently non-linear model of DC–DC converters results in some issues when trying to use linear controllers, such as the proportional–integral–derivative (PID) control for their regulation [17]. In fact, for the application of linear controllers, it is necessary first to linearize the system around the equilibrium point. Thus, the resulting response of the controller is only valid for a small region of operation around the equilibrium point. For this reason, in the recent literature, the focus has shifted towards using Lyapunov-based controllers for their regulation, because these techniques take model non-linearities into account [18,19]. Besides model non-linearities, the simulation of the DC–DC converter operation is affected by the uncertainty of the model parameters. In adaptive control, the aim is to estimate the uncertain plant parameters in real time and use these estimates to derive the input control law for the system. The adaptive control law tends to be based on Lyapunov techniques such as input–output feedback linearization [20] or input-state feedback linearization [21], which work by transforming the non-linear system into a linear one by a cancellation or a transformation mechanism. These mechanisms simplify the adaptive controller design but often lead to the cancellation of useful non-linearities [22,23].

Another main approach is the use of the backstepping technique [24], which is more flexible and does not force the system to appear linear. The backstepping technique can avoid the cancellation of useful non-linearities and often introduces additional nonlinear terms to improve the transient performance [25]. Further contributions address the control of switched systems described by a set of affine differential equations, based on a quadratic Lyapunov function, with applications on DC–DC converters [26] and develop a control law for power converters with affine models using hybrid dynamical systems theory [27].

Another form of adaptive control is the model reference adaptive control (MRAC) approach. The MRAC approach consists of a closed-loop controller that is capable of modifying the controller parameters to achieve asymptotic tracking of the reference trajectory provided as an input to the system [28]. The minimization of the error between the system output and the reference is achieved through the use of an adaptive mechanism. The structure of the adaptive mechanism is explicitly designed so that the trajectory to the equilibrium point is asymptotically stable. Additionally, the adaptive controller is also capable of providing effective means for shaping the transient performance, which allows different performance-robustness trade-offs. The above properties are satisfied by the Torelli Control Box (TCB) approach, which has been previously applied for the regulation of power systems, to solve power flow problems and mathematical programming problems [29–31]. The TCB approach has also been recently used to model switched capacitor converters whose dynamics are governed by Differential Algebraic Equations (DAE) instead of Ordinary Differential Equations (ODE) [32]. A further point is that in the Lyapunov-based control literature for the regulation of power converters, including model non-idealities that represent the internal losses of the components is not common [33,34]. The inclusion of parasitic parameters that model the internal losses makes the design of the resulting controller particularly complex but increases the precision and accuracy of actual results. On these bases, this paper presents a novel MRAC methodology based on the TCB approach to control the operation of DC–DC converters. In the proposed approach, the control variable used for the converters is the duty ratio, and the reference trajectory is specified for the output voltage. While considering the switched model with parasitic parameters, the control is based on the parameters of the averaged model. By using the PWM signal with sufficiently high frequency, the trajectories converge to an isolated fixed point, and the averaged system has a behaviour similar to the switching-mode converter [35].

Previous results have been reported for the control of an ideal Buck and Boost converter, highlighting the superiority of the results obtained over those found with a backstepping controller [36]. The main contributions of this paper are:

- The proposal of the MRAC-TCB controller applied to non-ideal Buck and Boost converters, taking into account inductor, capacitor and switching losses.
- The comparison of the results obtained from the novel controller with the results of controllers based on Feedback stabilization and Lyapunov redesign proposed in the literature for non-ideal Buck and Boost converters [37,38].
- The successful experimental verification of the behaviour of the MRAC-TCB controller on Buck and Boost converters.

This is the first time in which the proposed approach is used to show effective regulation of non-ideal power converter topologies.

The next sections of this paper are organized as follows. Section 2 shows the mathematical formulation for the MRAC-TCB approach. Section 3 demonstrates the application of the proposed approach for the regulation of the DC–DC Buck and Boost converters for tracking an output voltage reference while facing fluctuations in load and input voltages. This section also provides the comparison of the proposed controller with other Lyapunov-based controllers taken from the literature. Section 4 shows the experimental results on the two converter layouts controlled with the proposed approach. Finally, the last section contains the concluding remarks of the paper and indicates directions of future work.

2. Mathematical formulation of the MRAC-TCB approach

2.1. Description of the mathematical framework

Let us consider a non-linear algebraic differential equation system given by:

$$\dot{\mathbf{x}}(t) = \mathbf{f}(\mathbf{x}(t), \mathbf{u}(t)) \tag{1}$$

$$\mathbf{g}(\mathbf{x}(t)) - \mathbf{y}(t) = \mathbf{0} \tag{2}$$

where $\mathbf{x}(t)$, $\mathbf{u}(t)$ and $\mathbf{y}(t)$ are the vectors that contain the state variables, the control variables, and the algebraic variables, respectively, and t denotes time. Eq. (1) expresses the derivative in time of the state variables. Eq. (2) contains the algebraic equations.

The derivation of the TCB-based MRAC control approach can be broken down into three steps:

1. Design of a reference signal for the adaptive control law to follow.
2. Evaluation of the equilibrium point of the system and derivation of the reference trajectories for the state and input variables.
3. Derivation of a control law based on the TCB approach that forces the system trajectory to the reference trajectory.

In the first step, the reference signal for the control law is be designed to meet the specifications required for the system, such as rise time, settling time, overshoot, etc. [17].

The second step evaluates the reference trajectories of the state variables $\mathbf{x}$ and the control variables $\mathbf{u}$. The coordinates of the equilibrium point, denoted as ($\mathbf{x}^*$, $\mathbf{u}^*$), must satisfy the following equations:

$$\mathbf{f}(\mathbf{x}^*, \mathbf{u}^*) = \mathbf{0} \tag{3}$$

$$\mathbf{g}(\mathbf{x}^*) = \mathbf{y}_{r0} \tag{4}$$

where $\mathbf{y}_{r0}$ is defined as the vector that includes the main output variables considered as variables of interest.

The third step is the design of an adaptive control law that guarantees the asymptotic stability of equilibrium point. The adaptation mechanism is designed to allow minimization of following tracking errors with respect to the control signal $\mathbf{u}$:

$$\begin{aligned}\mathbf{e_x} &= \mathbf{W_x}(\mathbf{x}-\mathbf{x}^*)\\ \mathbf{e_u} &= \mathbf{W_u}(\mathbf{u}-\mathbf{u}^*)\\ \mathbf{e_f} &= \mathbf{f}(\mathbf{x},\mathbf{u})-\mathbf{f}(\mathbf{x}^*,\mathbf{u}^*)\end{aligned} \tag{5}$$

where $\mathbf{W_x}$ and $\mathbf{W_u}$ are diagonal matrices that contain the (positive) weights associated to each error referring to the state variables $\mathbf{x}$ and control variables $\mathbf{u}$, respectively. The term $\mathbf{f}(\mathbf{x}^*, \mathbf{u}^*)$ is null as it is estimated in an equilibrium point of the system.

Assuming $\mathbf{e} = [\mathbf{e}_\mathbf{x}^\mathrm{T}, \mathbf{e}_\mathbf{u}^\mathrm{T}, \mathbf{e}_\mathbf{f}^\mathrm{T}]^\mathrm{T}$, since the state vector $\mathbf{x}$ is $\mathbf{u}$-dependent, the controller design problem can be recast as follows:

$$\dot{\mathbf{x}}(\mathbf{u}) = \mathbf{f}(\mathbf{x}(\mathbf{u}),\mathbf{u}) \tag{6}$$

$$\mathbf{e}(\mathbf{x}(\mathbf{u}),\mathbf{u}) = \mathbf{0} \tag{7}$$

Therefore, the problem consists of evaluating the input vector $\mathbf{u}(t)$ such that each component of the error vector $\mathbf{e}$ is reduced to zero while simultaneously fulfilling the dynamic constraint given by (6).

A possible way to achieve this goal is based on the definition of the following Lyapunov function:

$$V = \frac{1}{2}\mathbf{e}^\mathrm{T}\mathbf{e} \tag{8}$$

which can be noticed to be a scalar positive semi-definite function. Now it should be noted that if the time derivative of the function V is proven to be negative definite (or negative semi-definite), then according to the Lyapunov theorem, the entries of the vector $\mathbf{e}(t)$ will asymptotically approach zero.

From (8) the time derivative of V can be evaluated as follows:

$$\dot{V} = \mathbf{e}^\mathrm{T}\dot{\mathbf{e}} \tag{9}$$

and because

$$\dot{\mathbf{e}} = \frac{\partial \mathbf{e}}{\partial \mathbf{u}}\dot{\mathbf{u}} \tag{10}$$

it results

$$\dot{V} = \mathbf{e}^\mathrm{T}\frac{\partial \mathbf{e}}{\partial \mathbf{u}}\dot{\mathbf{u}} \tag{11}$$

Now, enforcing the condition that $\dot{\mathbf{u}}$ changes according to the gradient of V:

$$\dot{\mathbf{u}}(t) = -K\left(\frac{\partial V}{\partial \mathbf{u}}\right)^\mathrm{T} = -K\left(\frac{\partial \mathbf{e}}{\partial \mathbf{u}}\right)^\mathrm{T}\mathbf{e} \tag{12}$$

where K is a positive constant, it follows:

$$\dot{V}(t) = -K\mathbf{e}^\mathrm{T}\left(\frac{\partial \mathbf{e}}{\partial \mathbf{u}}\right)\left(\frac{\partial \mathbf{e}}{\partial \mathbf{u}}\right)^\mathrm{T}\mathbf{e} \tag{13}$$

The expression (13) is a quadratic form that is surely negative semi-definite. This proves that to guarantee the asymptotic stability of the equilibrium point $\mathbf{x}^*$, the control signal $\mathbf{u}(t)$ must be generated according to (12). This in fact guarantees, with the asymptotic stability of V, the minimum of the error $\mathbf{e}$.

2.2. Interpretation of the MRAC-TCB approach

The MRAC-TCB approach adopts a non-standard adaptive control system. Starting from the initial conditions, the application of the MRAC-TCB approach requires:

1. The definition of a reference trajectory for the controlled variable. The reference trajectory is formed by the equilibrium points of the dynamic system. Because of that, the reference trajectory is an attractor of the controlled system. For the converters considered in this paper, the output variable is the average value of the output voltage, and the reference trajectory in our example is set to a given output voltage value.
2. The definition of a mechanism that allows the system to start from the initial conditions and approach the reference trajectory. For the converters considered in this paper, this mechanism consists of the definition of a Lyapunov function based on the error vector and on the assumption that the time derivative of the control variable changes according to the gradient of the Lyapunov function as in Eq. (12). The control signal is generated by defining suitable error functions with respect to the chosen reference trajectory. The error functions are then minimized by setting up an optimization procedure with dynamic constraints. Thereby, in the initial evolution, the controlled variable evolves towards the reference trajectory until it impacts on a value located onto the reference trajectory.
3. The definition of a mechanism that keeps the evolution of the system close to the reference trajectory after the reference trajectory has been approached. Since the reference trajectory contains the equilibrium points of the dynamic system, after impacting on the reference trajectory the resulting system must satisfy both the n-dimensional state dynamics of Eq. (1) and the n algebraic equations $\mathbf{f}(\mathbf{x},\mathbf{u}) = \mathbf{0}$. In this way, on the reference trajectory the system dynamics are reduced to the order n-n = 0, that is, the evolution on the reference trajectory is driven only by the reference signal [39]. Hence, the dynamics of the initial system are no longer followed, and the only dynamics are the ones imposed by the reference trajectory. Moreover, the dynamics on the reference trajectory are almost independent of parametric variations that occur in the system.

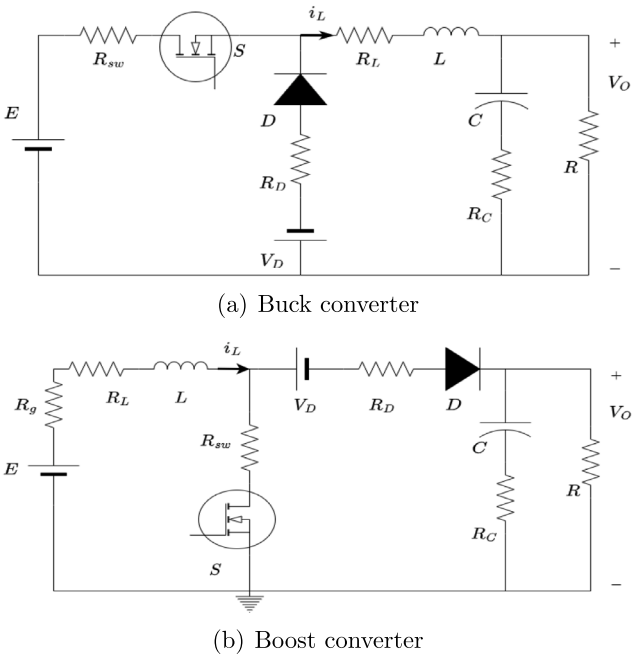

Fig. 1. DC–DC converter models with parasitic parameters: (a) Buck converter; (b) Boost converter.

For any variation that changes the system conditions, the response is given by the mechanism indicated at the point #2 above, that tends to drive the evolution of the system towards reaching the reference trajectory and remaining on that trajectory as explained at point #3 above. In this way, the system exhibits excellent convergence to the equilibrium points and adaptability to changes in the input variables.

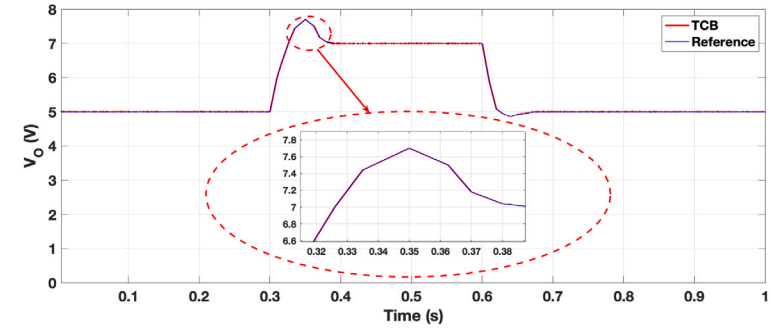

(a) Output voltage

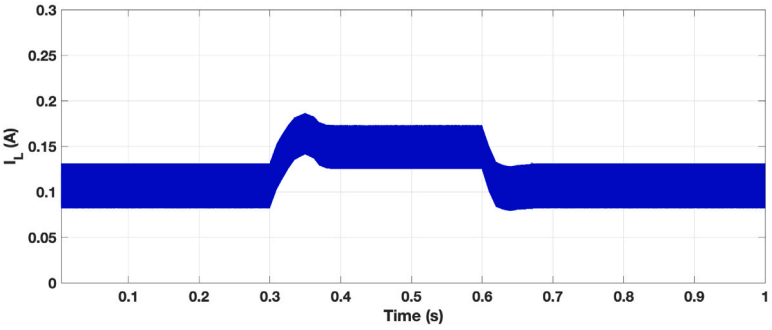

(b) Inductor current

Fig. 2. Output voltage and inductor current responses to the reference voltage tracking test for the Buck converter.

This approach has also been successfully used in systems with limit cycles [39].

Furthermore, the value of the gain factor K introduced in Eq. (12) affects the algorithm convergence. This can be inferred by analysing the dynamics of the tracking error function $\mathbf{e}(t)$ linked to the eigenvalues of the matrix $(\partial \mathbf{e}/\partial \mathbf{u})/(\partial \mathbf{e}/\partial \mathbf{u})^{\mathrm{T}}$, which are all real and positive. In general, from extensive testing it has been observed that the algorithm convergence will be improved by increasing the gain factor K within a small range. Anyway, beyond certain values, further increases of the gain factor K may result in slower convergence or, possibly, introduce oscillations. Commonly the gain factor K is chosen empirically as a function of the specific system.

3. Application to non-ideal buck and boost converter topologies

3.1. Steady state modelling of buck and boost converters with parasitic parameters

Different controllers have been designed for the regulation of DC–DC converter topologies. However, most of the work present in literature does not take into account the parasitic resistance referring to inductors, capacitors or switching losses. While it is true that the values of parasitic elements are relatively small, these values should not be ignored as they give rise to model uncertainties for practical implementation of the controllers [35]. Therefore, designing the controller by taking into account the parasitic elements of the converters is a key contribution of this paper.

Fig. 1 shows the Buck and Boost circuits with parasitic elements. The exact mathematical models for these converters have been taken from [37,40] for the Buck and Boost models, respectively. The large-signal dynamic model for the Buck and Boost converters, taking inductor, capacitor and switching non-linearities into account, can be derived using the volt-second and charge-second balance. In the notation used, E, x_1, x_2 and u represent the input voltage, inductor current, capacitor voltage and duty ratio, respectively. The non-ideal parameters R_{sw}, R_L, R_D, R_C and V_D are the switch resistance, inductor resistance, diode resistance, capacitor resistance and diode forward voltage drop, respectively.

In this paper, both converters are assumed to work in continuous conduction mode only.

The Buck converter model is formulated as:

$$\begin{cases} \dot{x}_1 = \dfrac{-1}{L}\left[((R_{sw} - R_D)u + R_D + R_L)x_1 + x_2 - u(E + V_D) + V_D\right] \\ \dot{x}_2 = \dfrac{x_1}{C} - \dfrac{x_2}{RC} \end{cases} \tag{14}$$

The Boost converter model is formulated as:

$$\begin{cases} \dot{x}_1 = \dfrac{1}{L}\left[-x_1(R_g + R_L) - x_1(1-u)\left(R_D + \dfrac{RR_C}{R+R_C}\right) + E \right. \\ \qquad \left. - x_2(1-u)\dfrac{R}{R+R_C} - x_1 R_{sw} u - V_D(1-u) \right] \\ \dot{x}_2 = (1-u)\dfrac{x_1}{C} - \dfrac{x_2}{RC} \end{cases} \tag{15}$$

3.2. Application of the MRAC-TCB control approach to the buck converter

As described in Section 2, the MRAC-TCB approach is applied following three steps.

In the first step, for simulation purposes, the reference signal for the regulation of the converter is generated graphically in Matlab and is directly sent as an input to the system. The system output y_{r0} is defined as the output voltage V_o. The vector of the state variable is $\mathbf{x} = \{x_1, x_2\}$, the control variable vector is $\mathbf{u} = \{u\}$, and the algebraic variable is $\mathbf{y} = \{y_{r0}\}$.

The second step is to derive the coordinates of the equilibrium point in the composite domain $(\mathbf{x}, \mathbf{u})$, denoted as $(\mathbf{x}^*, \mathbf{u}^*)$. For this purpose, the equilibrium point for the steady state values is derived by setting

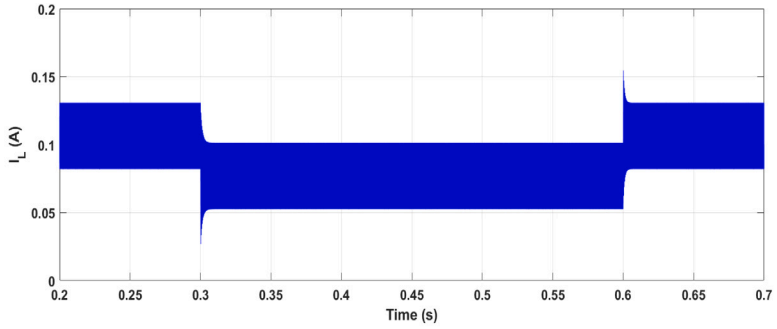

(a) Inductor current I_L

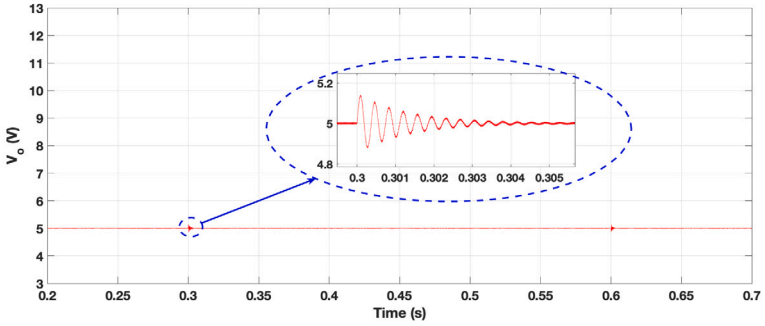

(b) Output voltage V_o

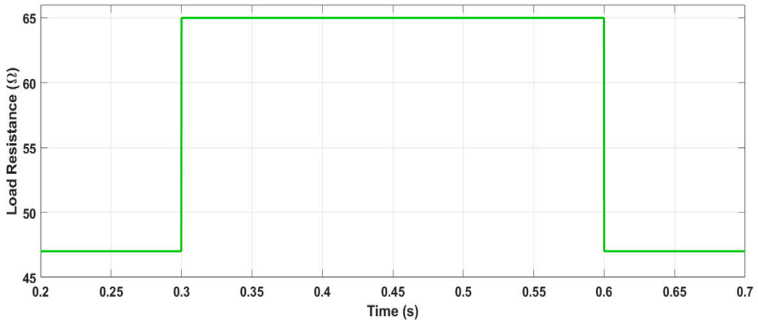

(c) Load resistance R

Fig. 3. Inductor current and output voltage responses to a load resistance variation from 47 Ω to 65 Ω in a given time interval for a Buck converter.

the contents of Eq. (14) to zero, obtaining:

$$\begin{cases} x_1^* = \frac{y_{r0}}{R} \\ x_2^* = y_{r0} \\ u^* = \frac{RV_D + y_{r0}(R+R_L+R_D)}{RV_D + y_{r0}(R_D - R_{sw}) + RE} \end{cases} \tag{16}$$

The third step is to design the adaptation mechanism for the minimization of the following tracking errors:

$$\begin{cases} e_{x_1} = w_{x_1}(x_1 - x_1^*) \\ e_{x_2} = w_{x_2}(x_2 - x_2^*) \\ e_u = w_u(u - u^*) \end{cases} \tag{17}$$

Based on Eq. (12) and the error vectors defined above, the expression for the control equation becomes:

$$\dot{u} = -K\left[\frac{dx_1}{du} w_{x_1}^2 (x_1 - x_1^*) + \frac{dx_2}{du} w_{x_2}^2 (x_2 - x_2^*) + w_u^2 (u - u^*)\right] \tag{18}$$

where K is the gain factor, with constant value, and w_{x_1}, w_{x_2} and w_u are weights defined on the variations of the state and control variables, respectively, with respect to the equilibrium point.

The sensitivity parameters $s_1 = \frac{dx_1}{du}$ and $s_2 = \frac{dx_2}{du}$ are calculated based on the Buck converter model given in Eq. (14):

$$\begin{cases} \dot{s}_1 = -\frac{1}{L}\left[s_1(uR_{sw} - uR_D + R_D + R_L) + s_2 + x_1(R_{sw} - R_D) - E - V_D\right] \\ \dot{s}_2 = \frac{1}{C}\left(s_1 - \frac{s_2}{R}\right) \end{cases} \tag{19}$$

3.3. Simulation results for the buck converter

The control has been simulated in the Matlab/Simulink environment. The converter parameters are specified in Table 1 along with the control parameters. The validity of the proposed control has been tested by considering three tests, with:

(i) reference voltage tracking,
(ii) output voltage regulation under varying load, and
(iii) output voltage regulation under input voltage variations.

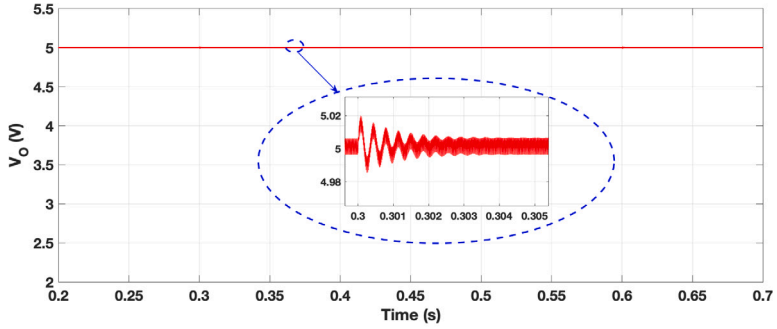

(a) Output voltage V_o

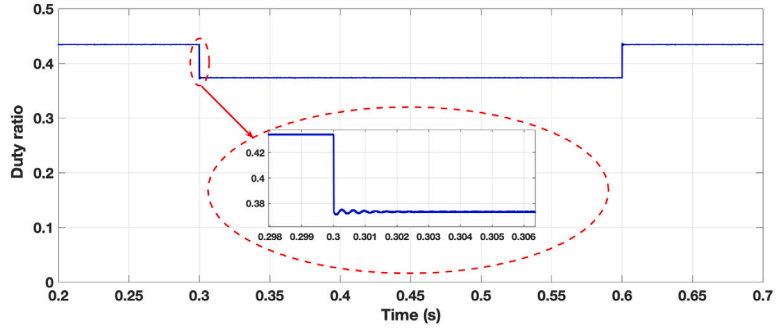

(b) Duty ratio u (control variable)

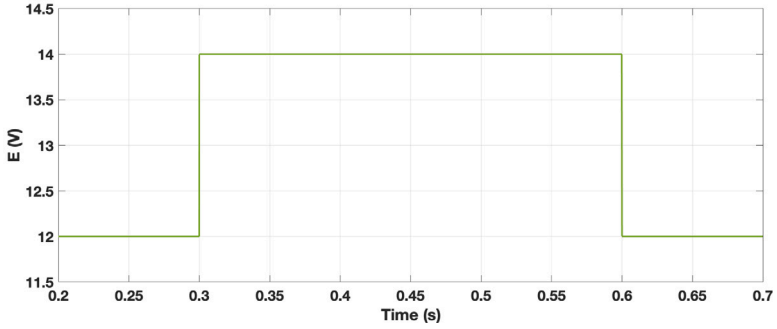

(c) Input Voltage Variation E

Fig. 4. Output voltage and duty ratio responses to an input voltage variation from 12 V to 14 V in a given time interval for a Buck converter.

Table 1
Specifications of Buck converter parameters and controller gain.

Description of parameters	Nominal value
Input voltage, E	12 V
Reference output voltage, V_o	5 V
Capacitance, C	10 uF
Inductance, L	1 mH
Load resistance, R	47 Ω
Switching frequency, f_s	62 kHz
Inductor resistance, R_L	0.15 Ω
Diode resistance, R_D	0.001 Ω
Switch resistance, R_{sw}	0.1 Ω
Diode forward voltage drop, V_D	0.4 V
TCB gain, K	10^4

The weights of the error terms in Eq. (17) are set as $w_{x_1} = 1$, $w_{x_2} = 2$, and $w_u = 3.0$. The results corresponding to the three tests are shown below.

3.3.1. Reference voltage tracking

As mentioned above, the goal of the MRAC-TCB controller is to track the reference voltage directly. For this purpose, the first task of the controller is to track the reference trajectory for the output voltage of the Buck converter. The reference is designed manually in Matlab using a signal builder. The results are shown in Fig. 2. From Fig. 2(a), the reference signal is designed to track a constant output voltage of 5 V with variations at $t = 0.3$ s and 0.6 s, respectively. Initially, the reference signal ensures that the nominal voltage is reached in less than one millisecond with maximum overshoot of 5.3 V (less than 6% of the nominal value). At $t = 0.3$ s, the reference voltage is increased to 7 V with rise time 20 ms, settling time (2%) of 65.5 ms, and maximum value 7.7 V. The reference is tracked with no steady-state error by the controller as shown by the zoom in Fig. 2(a) at t around 0.3 s. The reference signal is then brought back to the desired output voltage of 5 V with minimal overshoot and settling time. The output voltage again

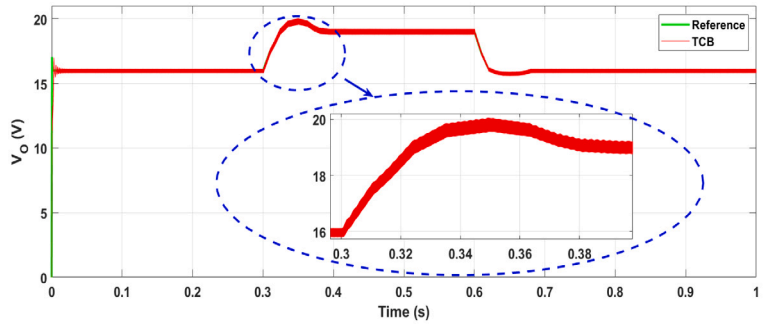

(a) Output voltage

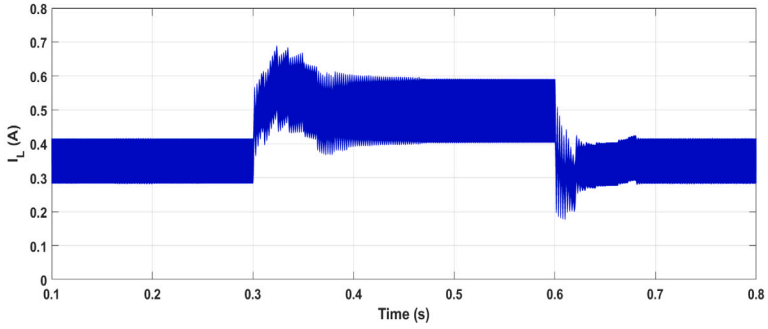

(b) Inductor current

Fig. 5. Output voltage tracking for the Boost converter.

tracks the reference almost perfectly. Fig. 2(b) shows the corresponding evolution of the inductor current.

3.3.2. Load resistance variations

The second test for the designed controller is the regulation of its output voltage when a step change in the specified load occurs. The reference output voltage for this test is specified to be 5 V. The nominal load resistance for the Buck converter is 47 Ω as mentioned in Table 1, but at time $t = 0.3$ s the load resistance steps up to 65 Ω and at time $t = 0.6$ s the load resistance is brought back to its initial value. The result of the load resistance variations on the inductor current and output voltage is shown in Fig. 3. From the figure, there is negligible steady-state error in either the inductor current or the output voltage. Furthermore, there is a maximum overshoot voltage of less than 2.67% and a settling time (2%) of only 470 μs.

3.3.3. Input voltage variations

The third test for the designed controller considers the input voltage variation. The input voltage is raised from the nominal 12 V to 14 V and the resulting changes in output voltage and duty ratio is shown in Fig. 4(a) and (b), respectively. In this test, overshoot voltage and settling time are remarkably small and almost negligible.

3.4. Application of the TCB control approach to the boost converter

To derive the equations of the MRAC-TCB based control for the Boost converter, the same methodology used for the Buck converter in the previous section is followed. The dynamic non-ideal model of Boost converter is given by Eq. (15). The reference signal is defined and is directly applied as an input for the simulation. The output voltage V_o is considered as the desired output y_{r0}. To derive the reference values at steady state, Eq. (15) is set to zero. The reference values are the same used in [40]:

$$\begin{cases} x_1^* = \frac{y_{r0}}{R(1-u^*)} \\ x_2^* = y_{r0} \\ u^* = \\ \frac{E}{V_o}\frac{1+\frac{y_{r0}}{E}\left(\frac{R_{SW}-R_D-R\|R_C}{R}\right)+\sqrt{\left(1+\frac{y_{r0}}{E}\left(\frac{R_{SW}-R_D-R\|R_C}{R}\right)\right)^2-4\left(\frac{y_{r0}}{E}\right)^2\left(\frac{R}{R+R_C}+\frac{V_D}{y_{r0}}\right)\left(\frac{R_E+R_L+R_{SW}}{R}\right)}}{2\left(\frac{R}{R+R_C}+\frac{V_D}{y_{r0}}\right)} \end{cases} \tag{20}$$

The errors to be minimized using the adaptation mechanism are defined as:

$$\begin{cases} e_{x_1} = w_{x_1}(x_1 - x_1^*) \\ e_{x_2} = w_{x_2}(x_2 - x_2^*) \\ e_u = w_u(u - u^*) \end{cases} \tag{21}$$

The control equation for the Boost converter is also the same as the one used for the Buck converter, based on Eq. (12):

$$\dot{u} = -K\left[\frac{dx_1}{du}w_{x_1}^2(x_1 - x_1^*) + \frac{dx_2}{du}w_{x_2}^2(x_2 - x_2^*) + w_u^2(u - u^*)\right] \tag{22}$$

where K is a constant positive gain factor and the weights are calculated empirically.

The sensitivity parameters $s_1 = \frac{dx_1}{du}$ and $s_2 = \frac{dx_2}{du}$ are calculated based on the original Boost converter model given in Eq. (15). The

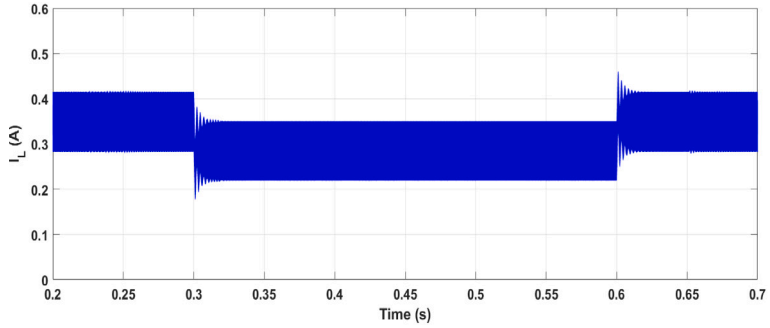

(a) Inductor current I_L

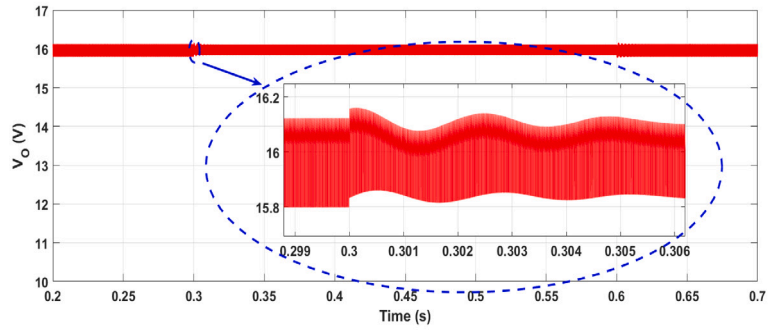

(b) Output voltage V_o

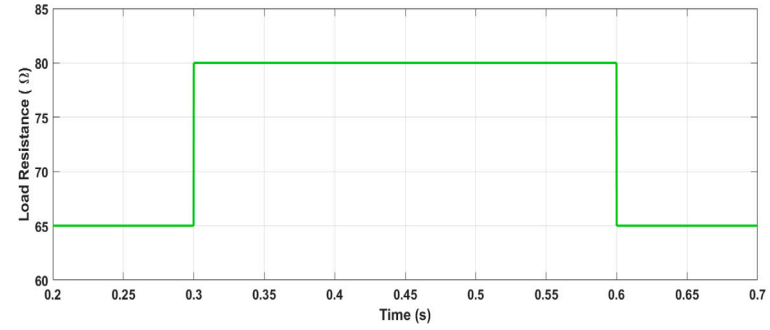

(c) Load resistance R

Fig. 6. Inductor current (a) and output voltage response (b) corresponding to the load resistance variation (c) from 65 Ω to 80 Ω in a given time interval for the Boost converter.

equations for deriving the sensitivity parameters are:

$$\begin{cases} \dot{s}_1 = -\frac{s_1}{L}(R_g + R_L + uR_{sw} + a(1-u)) \\ \quad -\frac{s_2}{L}((1-u)\frac{R}{R+R_C}) - \frac{x_1}{L}(-a + R_{sw}) \\ \quad +\frac{V_D}{L} + \frac{Rx_2}{L(R+R_C)} \\ \dot{s}_2 = -\frac{s_1}{C} - \frac{s_2}{RC} \end{cases} \tag{23}$$

where $a = \frac{RR_C}{R+R_C} + R_D$

3.5. Simulation results for the boost converter

The simulations for the Boost converter were coded and executed in Matlab/Simulink. The specifications for the Boost converter and the controller gains K are indicated in Table 2. The weights used for the error terms in Eq. (21) are empirically set to $w_{x_1} = 1$, $w_{x_2} = 1$, and $w_u = 3.5$, to compensate for the differences in the corresponding quantities.

The performance of the proposed controller has been tested by considering three tests, with:

Table 2
Specifications of boost converter parameters and controller gain.

Description of parameters	Nominal value
Input voltage, E	12 V
Reference output voltage, V_o	16 V
Capacitance, C	470 μF
Inductance, L	270 μH
Load resistance, R	65 Ω
Switching frequency, f_s	62 kHz
Inductor resistance, R_L	0.125 Ω
Switch resistance, R_{sw}	0.08 Ω
Input resistance, R_g	0.2 Ω
Diode forward voltage drop, V_D	0.3 V
TCB gain, K	10^3

(i) reference voltage tracking,
(ii) output voltage regulation under varying load, and
(iii) output voltage regulation under input voltage variations.

The results corresponding to the three tests are shown below.

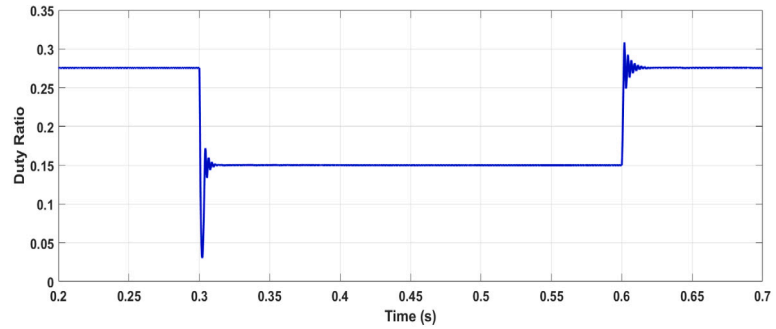

(a) Duty ratio u (control variable)

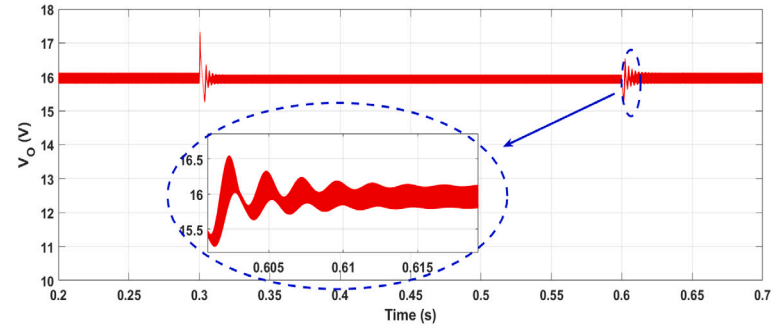

(b) Output voltage V_o

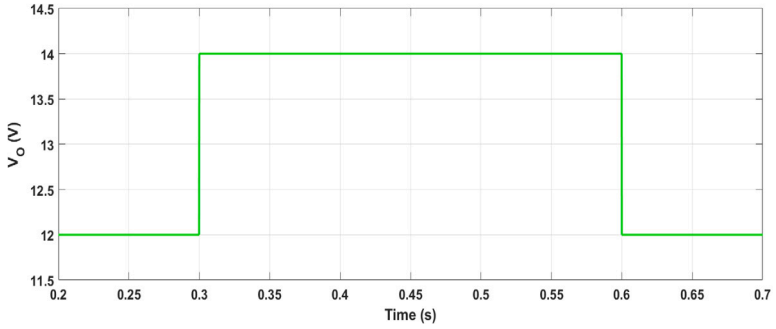

(c) Input voltage variation E

Fig. 7. Duty ratio and output voltage response to the input voltage variation from 5 V to 7 V in a given time interval for the Boost converter.

3.5.1. Reference voltage tracking

As in the case of the Buck converter, a similar reference is used for the Boost converter. The Boost converter nominal voltage for reference tracking is 16 V, but at time $t = 3$ s the voltage is stepped up to 19 V. This voltage is then stepped down to 16 V at $t = 0.6$ s. The initial time to reach the steady state for reference is designed to be 1.875 ms. Then at $t = 3$ s, the voltage is stepped up to 19 V. As seen from Fig. 5(a), the reference is tracked with negligible steady state error and reaches a settling time (2%) of 12 ms and a peak overshoot of 20.04 V. The evolution of the inductor current is shown in Fig. 5(b).

3.5.2. Load resistance variations

The aim of the second test is to maintain a constant voltage at the output of the converter while the Boost converter is subject to variations in the load resistance. The nominal load value, as mentioned in Table 2, is 65 Ω. This load value is changed to 80 Ω at time $t = 0.3$ s and is brought back to the nominal value at $t = 0.6$ s. The results are shown in Fig. 6.

From Fig. 6, there is negligible steady state error before or after the load resistance step up. The voltage variations are tiny. From Fig. 6(a), the rise time and settling time (2%) for the current can be calculated as 3305 μs and 298 μs, respectively.

3.5.3. Input voltage variations

For this test, the aim is to maintain a constant voltage at the Boost converter output while the input voltage is subject to variations. The nominal input voltage is 12 V, is changed to 14 V at time $t = 0.3$ s, and is brought back to the nominal value at $t = 0.6$ s. The results are shown in Fig. 7.

From Fig. 7, it can be noted that there is no steady state error before or after the input voltage step up. The large voltage variations are due to the consideration of non-idealities in the Boost converter model. From Fig. 7(a), the rise time and settling time (2%) for the current can be calculated as 754 ms and 816 ms, respectively.

3.6. Comparison with other controllers

For comparison purposes, the results of our proposed controllers have been compared with other controllers derived in literature for non-ideal Buck and Boost converters. The controls presented in the papers taken from the literature have been replicated exactly as proposed.

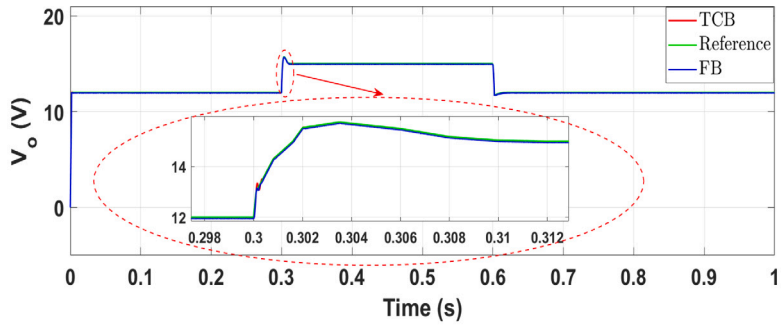

(a) Output voltage reference tracking

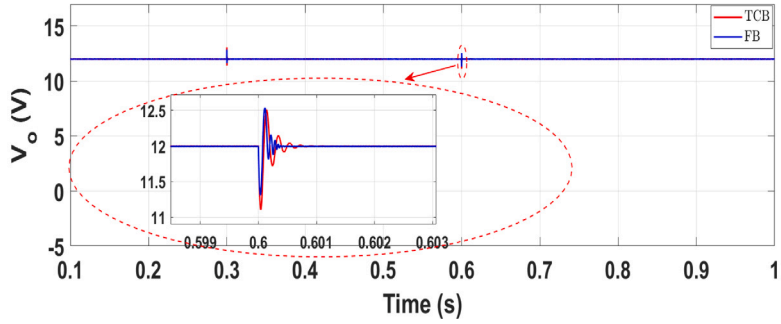

(b) Output voltage regulation under load variation

Fig. 8. Comparison between the MRAC-TCB and the Feedback stabilization controls of a Buck Converter under different conditions.

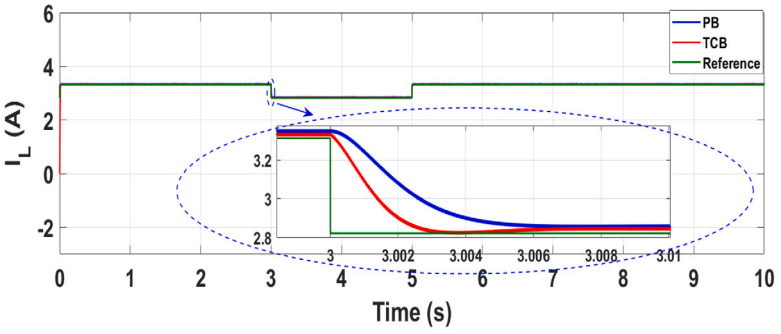

(a) Inductor current

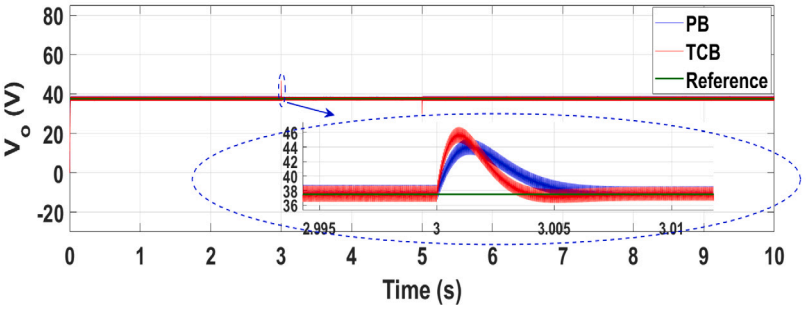

(b) Output Voltage

Fig. 9. Inductor current and Output voltage response comparisons due to load variations for the Boost converter.

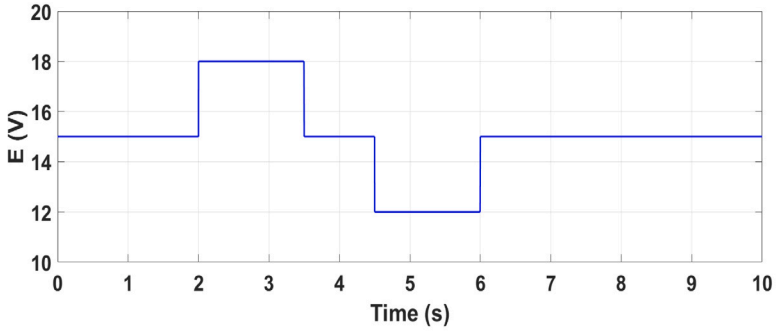

(a) Input Voltage

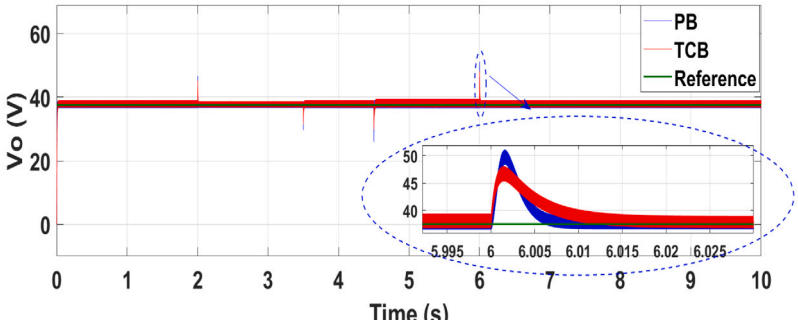

(b) Output Voltage

Fig. 10. Output voltage response comparisons due to fluctuations in the input voltage for the Boost converter.

The parameters of the converter and controller to which the MRAC-TCB control is applied have been modified to produce comparable results.

For the Buck converter, comparison of the MRAC-TCB control is provided with respect to another non-linear control technique proposed in [37]. The testing of the controller has been done under voltage reference tracking and load resistance variations. The results are shown in Fig. 8. Both the MRAC-TCB controller and the Extended Feedback (FB) stabilization-based controller have good comparable results under the operating conditions considered. In Fig. 8(a), both controllers follow the desired output voltage with no overshoot or steady state errors. In Fig. 8(b), the results are presented when the load resistance is varied from 10 Ω to 15 Ω and then brought back to the original value. The nominal output voltage is 12 V, as specified in Table I from [37].

Similarly, for the Boost converter, for comparison purposes the results obtained from MRAC-TCB have been compared with the results reached with the Passivity-Based (PB) controller proposed in [38]. For the first test, the load resistance is varied from 30 Ω to 35 Ω at $t = 3$ s and is then brought back to 30 Ω at $t = 5$ s. The corresponding changes in the inductor current and output voltage are shown in Fig. 9.

The other test is the input voltage variation test, for which a fluctuating input voltage is considered, as shown in Fig. 10(a). The corresponding response in the output voltage can be seen in Fig. 10(b). As seen from the figure, despite the strong and frequent fluctuations in the input voltages, both controllers are able to track the reference voltage with very low settling time and no steady state errors.

4. Experimental results

The performance of the proposed controllers has been validated by setting up an experimental testing with Buck and Boost converters. The main parameters of the converters are the same used in the simulations presented in the previous sections. The converters have been constructed on dedicated circuit boards. The Arduino microcontroller is used for implementing the controller in the hardware. For the measurements, the digital oscilloscope used is Teledyne LeCroy wavesurfer 3024z with 200 MHz bandwidth and 4 GS/s sampling rate.

The results of the experimental tests are shown in the next subsections.

4.1. Buck converter

Fig. 11 shows the experimental setup prepared to control a MOSFET-based Buck converter, with physical components implemented on a dedicated Buck converter board, the Arduino microcontroller board, and the control system driven through the Matlab/Simulink platform. The electronic load used has an equivalent resistance of 47 Ω. The location of the points used for the voltage and current measurements with the corresponding probes is indicated in Fig. 11. Fig. 12 reports the inductor current for a few switching periods. The switching frequency is 62.5 kHz. The experimental waveforms of the input and output voltages are presented in Fig. 13, for successive changes in the input voltage. It has to be noticed that the vertical scale referring to the output voltage is amplified ten times with respect to the vertical scale that shows the input voltage, and also in this case the changes in the output voltage after each variation of the input voltage are tiny. Thereby, the output voltage practically adapts to the reference trajectory very quickly, confirming the excellent properties of the proposed MRAC-TCB controller.

Fig. 14 shows the waveforms of the relevant experimental quantities on the Matlab/Simulink side control features. The successive changes in the input voltage are shown in Fig. 14(a). Correspondingly, in Fig. 14(b), the output voltage shows a quick variation and goes back to the reference value, indicating the fast adaptation of the proposed MRAC-TCB control. Note that starting from a solution that is close to

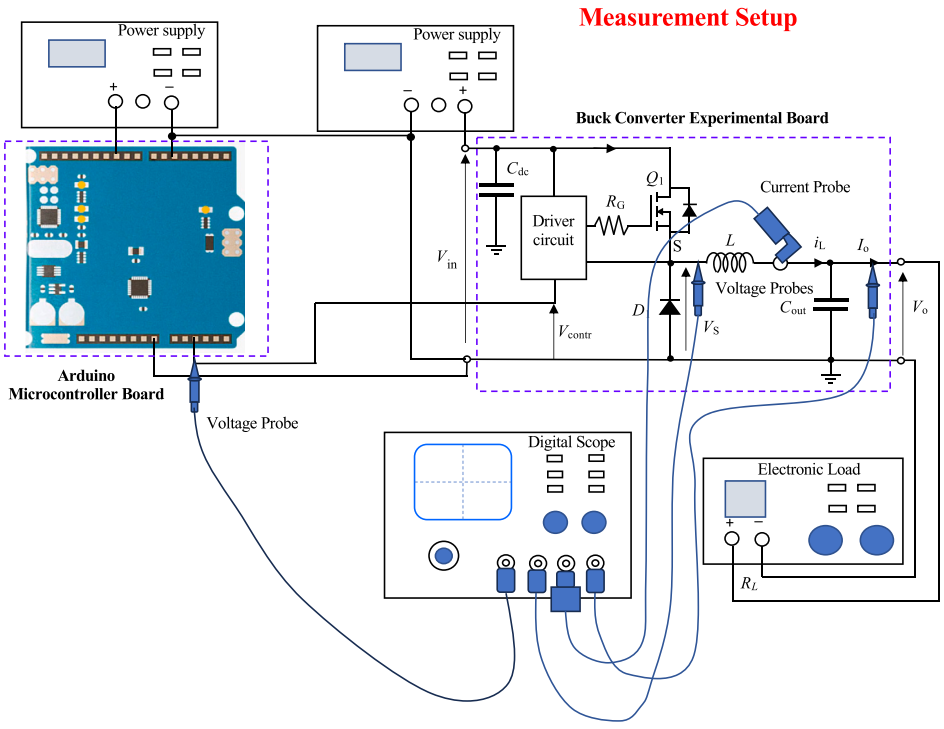

Fig. 11. Experimental setup of the circuits for controlling the Buck converter.

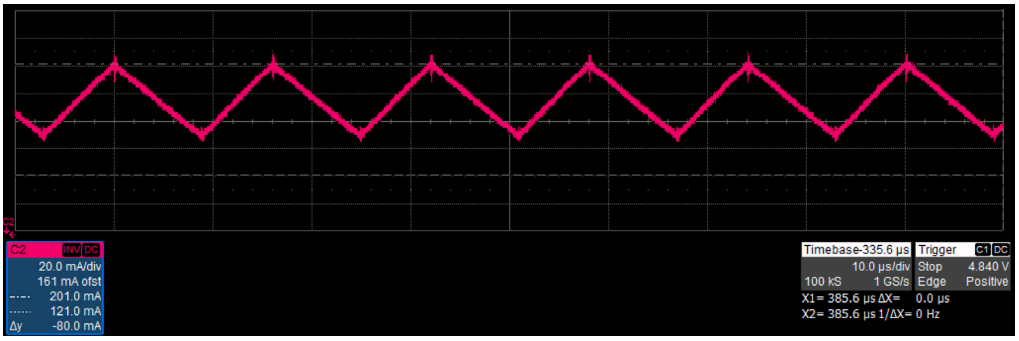

Fig. 12. Experimental waveform of the inductor current at steady state in the Buck converter operated under MRAC-TCB control.

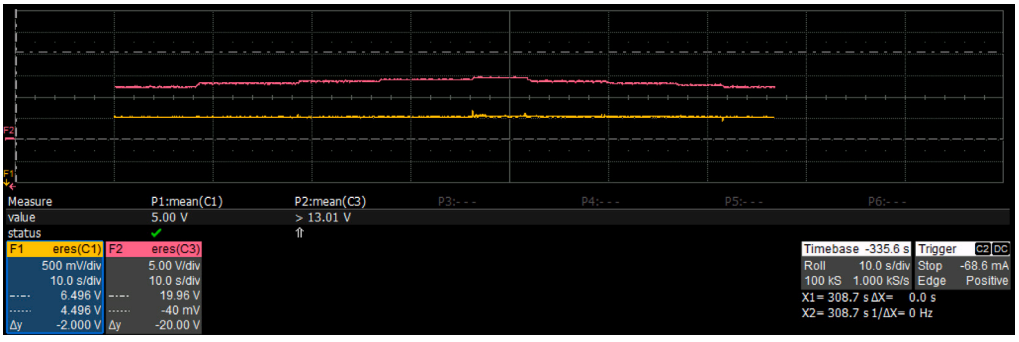

Fig. 13. Experimental waveforms for the input and output voltages in the Buck converter operated under MRAC-TCB control. The upper line is the input voltage, with vertical scale 5 V/division. The lower line is the output voltage, with vertical scale expanded to 0.5 V/division.

the reference, the output voltage impacts the reference trajectory very fast and remains then close to the reference trajectory. The duty ratio resulting during the experimental test is reported in Fig. 14(c), showing how the adaptability of the duty ratio contributes to keeping the output voltage close to the reference value.

4.2. Boost converter

The experimental testing on the Boost converter has been carried out with a similar setup, shown in Fig. 11, by replacing the Buck converter experimental board with the Boost converter experimental board.

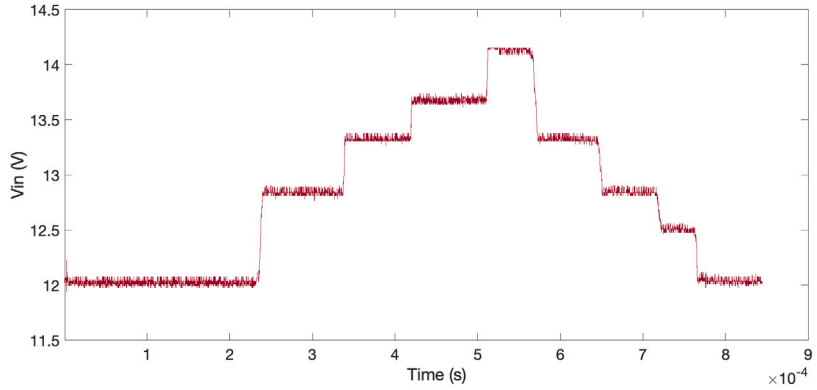

(a) Input voltage

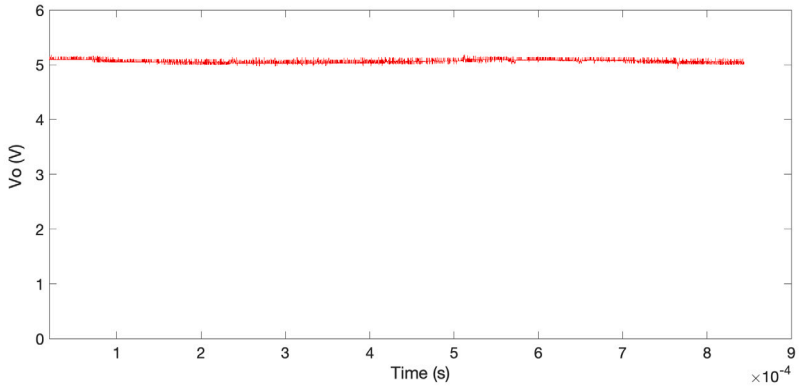

(b) Output voltage

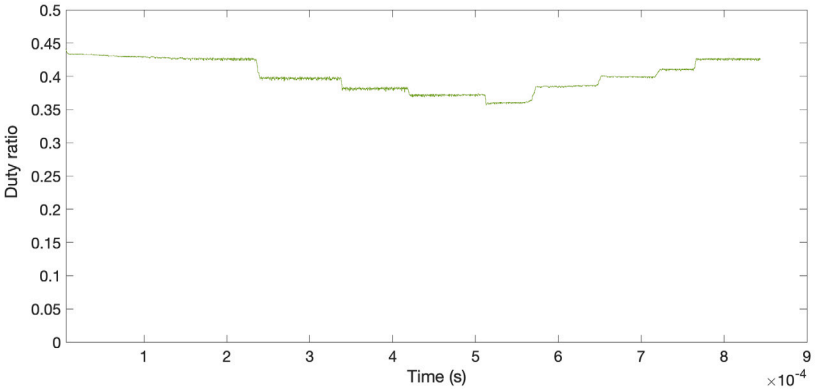

(c) Duty ratio

Fig. 14. Waveforms taken from the Matlab-Simulink side during the experimental test on the Buck converter.

The experimental waveforms of the input and output voltages are presented in Fig. 15, for successive changes in the input voltage. After each variation of the input voltage, the output voltage quickly follows the reference trajectory with a very small initial variation. Also in this case, the output voltage adapts to the reference trajectory very quickly, confirming the excellent properties of the proposed MRAC-TCB controller.

Fig. 16 shows the waveforms of the relevant quantities seen on the Matlab-Simulink side. The successive changes in the input voltage are shown in Fig. 16(a), while the output voltage (Fig. 16(b)) remains close to the reference trajectory. Fig. 16(c) shows that the duty ratio resulting during the experimental test corresponds to the calculated values.

5. Conclusion

In this paper, a new control methodology has been proposed for the regulation and adaptive reference tracking of DC/DC power electronic converters. The controller has been developed by using a model reference adaptive control methodology whose control mechanism is based on the Torelli Control Box methodology. The asymptotic stability of the controller is guaranteed by the Lyapunov stability criterion. The controller has been applied for the first time to non-ideal Buck and Boost converter topologies with the inclusion of the model non-linearities. Considering the model non-linearities makes the control system more complex, however, it is necessary for obtaining accurate regulation

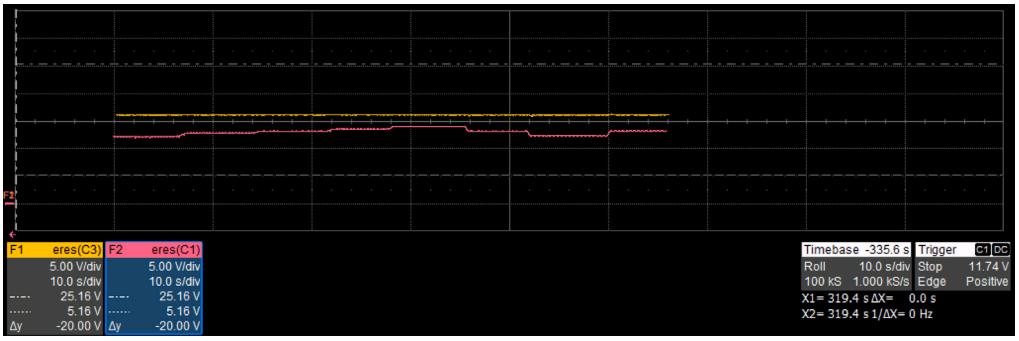

Fig. 15. Experimental waveforms for the input and output voltages in the Boost converter operated under MRAC-TCB control. The upper line is the output voltage. The lower line is the input voltage.

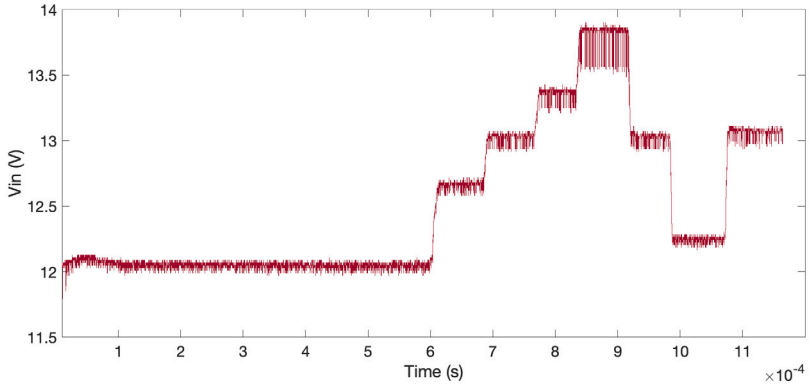

(a) Input voltage

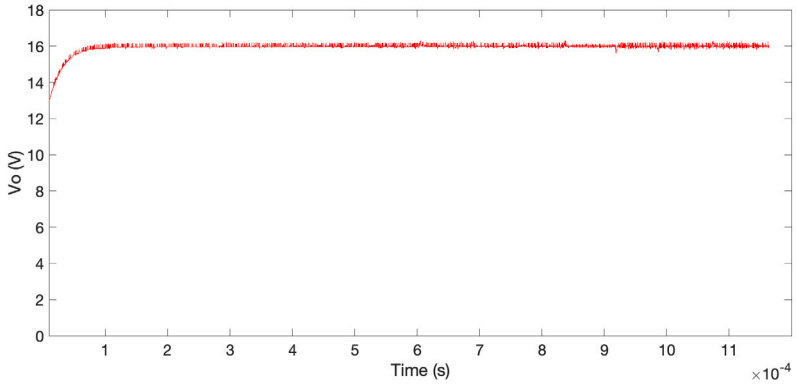

(b) Output voltage

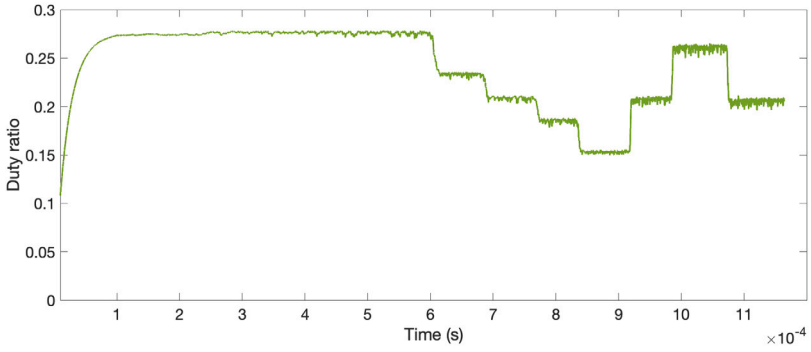

(c) Duty ratio (output)

Fig. 16. Waveforms taken from the Matlab-Simulink side during the experimental test on the Boost converter.

of these converters. The application of the proposed controller to the Buck and Boost converters has also been tested in experimental cases, showing the remarkable effectiveness of the proposed control methodology. For comparison purposes, simulations have been carried out between the proposed controller and other controllers proposed in the literature. From the results, the proposed controller has provided comparable or superior results under the same testing conditions.

This paper has given the mathematical foundations for successive use of the proposed controller in the power electronics domain. The work in progress is dedicated to extend the development of the proposed control principle to other power electronic converters.

CRediT authorship contribution statement

Muhammad Ahmed Qureshi: Conceptualization, Methodology, Software, Writing – original draft, Writing – review & editing. **Salvatore Musumeci:** Conceptualization, Methodology, Writing – original draft, Writing – review & editing. **Francesco Torelli:** Conceptualization, Methodology, Writing – original draft, Writing – review & editing. **Alberto Reatti:** Conceptualization, Methodology, Writing – original draft, Writing – review & editing. **Andrea Mazza:** Conceptualization, Methodology, Writing – original draft, Writing – review & editing. **Gianfranco Chicco:** Conceptualization, Methodology,Validation, Writing – original draft, Writing – review & editing.

Declaration of competing interest

The authors declare that there is no conflict of interest for this paper.

Data availability

Data will be made available on request.

References

[1] Wang J, Wang B, Zhang L, Wang J, Shchurov N, Malozyomov B. Review of bidirectional DC–DC converter topologies for hybrid energy storage system of new energy vehicles. Green Energy Intell Transp 2022;1(2):100010.

[2] Alavi O, Rajabloo T, De Ceuninck W, Daenen M. Non-isolated DC-DC converters in fuel cell applications: Thermal analysis and reliability comparison. Appl Sci 2022;12(10):5026.

[3] Cavallaro C, Musumeci S, Santonocito C, Pappalardo M. Smart photovoltaic UPS system for domestic appliances. In: 2009 international conference on clean electrical power. IEEE; 2009, p. 699–704.

[4] Eguchi K, Kuwahara K, Ishibashi T. Analysis of an LED lighting circuit using a hybrid buck–boost converter with high gain. Energy Rep 2020;6:250–6.

[5] Sutikno T, Purnama HS, Widodo NS, Padmanaban S, Sahid MR. A review on non-isolated low-power DC–DC converter topologies with high output gain for solar photovoltaic system applications. Clean Energy 2022;6(4):557–72.

[6] Steigerwald RL, De Doncker RW, Kheraluwala H. A comparison of high-power DC-DC soft-switched converter topologies. IEEE Trans Ind Appl 1996;32(5):1139–45.

[7] Chewale MA, Wanjari RA, Savakhande VB, Sonawane PR. A review on isolated and non-isolated DC–DC converter for PV application. In: 2018 international conference on control, power, communication and computing technologies. IEEE; 2018, p. 399–404.

[8] Alam M, Kumar K, Dutta V. Comparative efficiency analysis for silicon, silicon carbide MOSFETs and IGBT device for DC–DC boost converter. SN Appl Sci 2019;1(12):1–11.

[9] Buschendorf M, Weber J, Bernet S. Comparison of the IGCT and IGBT for the modular multilevel converter in HVDC applications. In: Derbel F, Derbel N, Kanoun O, editors. Power Syst Smart Energies. Berlin, Boston: De Gruyter Oldenbourg; 2017, p. 67–82. http://dx.doi.org/10.1515/9783110448412-005.

[10] Prado EO, Bolsi PC, Sartori HC, Pinheiro JR. An overview about Si, superjunction, SiC and GaN power MOSFET technologies in power electronics applications. Energies 2022;15(14):5244.

[11] Musumeci S, Mandrile F, Barba V, Palma M. Low-voltage GaN FETs in motor control application; issues and advantages: a review. Energies 2021;14(19):6378.

[12] Hossain M, Rahim N, et al. Recent progress and development on power DC-DC converter topology, control, design and applications: A review. Renew Sustain Energy Rev 2018;81:205–30.

[13] Sharma P, Dhaked DK, Sharma AK. Mathematical modeling and simulation of DC-DC converters using state-space approach. In: Proceedings of second international conference on smart energy and communication. Springer; 2021, p. 11–29.

[14] Reatti A, Kazimierczuk MK. Small-signal model of PWM converters for discontinuous conduction mode and its application for boost converter. IEEE Trans Circuits Syst I 2003;50(1):65–73.

[15] Mohammadian L, Babaei E, Sharifian MBB. Buck-boost dc-dc converter control by using the extracted model from signal flow graph method. Int J Appl Math Electron Comput 2015;3(3):155–60.

[16] Ozbay H. Comparison of sliding mode and fuzzy logic MPPT techniques for PV systems. Electron Lett Sci Eng 2020;16(1):26–35.

[17] Kazimierczuk MK. Pulse-width modulated DC-DC power converters. John Wiley & Sons; 2015.

[18] Reatti A, Balzani M. PWM switch model of a buck-boost converter operated under discontinuous conduction mode. In: 48th midwest symposium on circuits and systems. IEEE; 2005, p. 667–70.

[19] Salimi M, Zakipour A. Lyapunov based adaptive-robust control of the non-minimum phase DC-DC converters using input-output linearization. J Power Electron 2015;15(6):1577–83.

[20] Tang M, Cao J, Yang X, Wang X, Gu B. Model reference adaptive control based on Lyapunov stability theory. In: The 26th Chinese control and decision conference. IEEE; 2014, p. 1828–33.

[21] Cervone A, Brando G. Input-state feedback linearization of a boost DC/DC converter. In: ELECTRIMACS 2019. Springer; 2020, p. 139–53.

[22] Wu J, Lu Y. Feedback linearization adaptive control for a buck converter with constant power loads. In: 2018 IEEE international power electronics and application conference and exposition. IEEE; 2018, p. 1–6.

[23] Corti F, Laudani A, Lozito GM, Reatti A, Bartolini A, Ciani L, et al. Modelling of a pulse-skipping modulated DC–DC buck converter. IET Power Electron 2022.

[24] Yin Y, Liu J, Wang S, Lin H, Vazquez S, Zeng Q, et al. Backstepping control of a DC-DC boost converters under unknown disturbances. In: IECON 2018-44th annual conference of the IEEE Industrial Electronics Society. IEEE; 2018, p. 1055–60.

[25] Boutebba O, Semcheddine S, Krim F, Corti F, Reatti A, Grasso F. A nonlinear back-stepping controller of DC-DC non inverting buck-boost converter for maximizing photovoltaic power extraction. In: 2020 IEEE international conference on environment and electrical engineering and 2020 IEEE industrial and commercial power systems Europe. IEEE; 2020, p. 1–6.

[26] Albea C, Garcia G, Zaccarian L. Hybrid dynamic modeling and control of switched affine systems: application to DC-DC converters. In: 2015 54th IEEE conference on decision and control. IEEE; 2015, p. 2264–9.

[27] Albea C, Sferlazza A, Gordillo F, Gómez-Estern F. Control of power converters with hybrid affine models and pulse-width modulated inputs. IEEE Trans Circuits Syst I Regul Pap 2021;68(8):3485–94.

[28] Ardhenta L, Subroto RK. Application of direct MRAC in PI controller for DC-DC boost converter. Int J Power Electron Drive Syst 2020;11(2):851.

[29] Torelli F, Montegiglio P, De Bonis A, Catalão JP, Chicco G, Mazza A. A new approach for solving DAE systems applied to distribution networks. In: 2014 49th international universities power engineering conference. IEEE; 2014, p. 1–6.

[30] Torelli F, Vaccaro A, Xie N. A novel optimal power flow formulation based on the Lyapunov theory. IEEE Trans Power Syst 2013;28(4):4405–15.

[31] De Bonis A, Catalão JP, Mazza A, Chicco G, Torelli F. A novel optimization algorithm solving network reconfiguration. In: 2014 power systems computation conference. IEEE; 2014, p. 1–7.

[32] Ernst H, Gerhard W. Solving ordinary differential equations II: Stiff and differentialalgebraic problems. New York: Springer-Verlag; 1996.

[33] Faifer M, Piegari L, Rossi M, Toscani S. An average model of DC–DC step-up converter considering switching losses and parasitic elements. Energies 2021;14(22):7780.

[34] Qureshi MA, Musumeci S, Torelli F, Reatti A, Mazza A, Chicco G. Application of a novel adaptive control approach for the regulation of power converters. In: 2022 57th international universities power engineering conference. IEEE; 2022, p. 1–6.

[35] Baldi S, Papachristodoulou A, Kosmatopoulos EB. Adaptive pulse width modulation design for power converters based on affine switched systems. Nonlinear Anal Hybrid Syst 2018;30:306–22.

[36] Zhang Z, Song G, Zhou J, Zhang X, Yang B, Liu C, et al. An adaptive backstepping control to ensure the stability and robustness for boost power converter in DC microgrids. Energy Rep 2022;8:1110–24.

[37] Csizmadia M, Kuczmann M. Extended feedback linearisation control of non-ideal DCDC buck converter in continuous-conduction mode. Power Electron Drives 2022;7(1):1–8.

[38] Mihaly V, Susca M, Dobra P. Passivity-based controller for nonideal DC-to-DC boost converter. In: 2019 22nd international conference on control systems and computer science. (CSCS), IEEE; 2019, p. 30–5.

[39] Piccinni G, Torelli F, Avitabile G. Chaos suppression in forced chaotic systems by innovative sliding mode control. IEEE Trans Circuits Syst II Express Briefs 2020;67(8):1424–8.

[40] Siddhartha V, Hote YV. Systematic circuit design and analysis of a non-ideal DC–DC pulse width modulation boost converter. IET Circuits Devices Syst 2018;12(2):144–56.